Advances in Geo-Energy Research

Vol. 15, No. 3, p. 203-215, 2025

Original article

Simulation and optimization of a coupled reservoir and multi-phase flow network model

Paul Roger Leinan[1]*, Torgeir Stensrud Ustad[1], Stein Krogstad[2], Thiago Lima Silva[3], Miguel Muñoz Ortiz[3], Lars Hellemo[3], Ivar Eskerud Smith[1]

[1]*SINTEF Industry, Process Technology, Trondheim 7034, Norway*

[2]*SINTEF Digital, Mathematics and Cybernetics, Oslo 0373, Norway*

[3]*SINTEF Industry, Sustainable Energy Technology, Trondheim 7034, Norway*

Keywords:
Model coupling
optimization
model reduction
MRST

Cited as:
Leinan, P. R., Ustad, T. S., Krogstad, S., Silva, T. L., Ortiz, M. M., Hellemo, L., Smith, I. E. Simulation and optimization of a coupled reservoir and multi-phase flow network model. Advances in Geo-Energy Research, 2025, 15(3): 203-215.
https://doi.org/10.46690/ager.2025.03.04

Abstract:
This work considers a coupled system of the MATLAB Reservoir Simulation Toolbox, a multi-phase network simulator and topside processing facilities, with the intent to provide a research tool for studying integrated planning and optimization. To this end, a collection of open-source tools are presented that can be combined with MATLAB Reservoir Simulation Toolbox to model, evaluate and optimize the economy of integrated systems, including reservoir and network under different market (costs and revenue) scenarios. The tools are organized in four repositories containing code for cost/price scenario modelling, derivative-free trust region optimization, pipe/network simulation and reservoir-network coupling and examples. A brief background on each of these tools is given, followed by the presentation of a fully implicit approach for the reservoir-network coupling. Moreover, a description is given on how to set up coupled simulation models, and finally, a presentation of numerical examples, including an optimization example that utilizes the full set of above-mentioned tools.

1. Introduction

The upstream part of the hydrocarbon value chain, from reservoir to export, involves multiple disciplines and a wide range of process and production technologies. Optimization of the system as a whole is therefore a challenge, given: the complexities of modelling the coupled system, the significantly different timescales for the flow through the system, the uncertainty regarding the detailed reservoir structure, the uncertainty of future profits and costs trajectories.

Additionally, the operation priorities change during the lifetime of a petroleum field. For example, reservoir pressure support and produced water strategies may only become important in the later stages of the field lifetime, while in the early stage of development a frequent drilling schedule may be cost effective, due to the high initial production potential. These complexities and uncertainties in combination with the inherent high profitability of hydrocarbon production may have dampened the incentives to implement system wide optimization over both short-term (days to weeks) and, especially, long-term (years). However, given the current focus on reduced carbon footprints this work focuses on developing a computationally efficient system optimization framework, where the influence of uncertainty can readily be implemented. The aim is optimal policies for hydrocarbon field operation that maximizes profit and minimizes the energy consumption and emissions.

Different models are employed in the optimization depending on the time scale of decisions, and there is a natural divi-

Yandy Scientific Press

*Corresponding author.
E-mail address: paul.roger.leinan@sintef.no (P. R. Leinan); Torgeir.Ustad@sintef.no (T. S. Ustad); Stein.Krogstad@sintef.no (S. Krogstad); Thiago.Silva@sintef.no (T. L. Silva); miguel.ortiz@sintef.no (M. M. Ortiz); Lars.Hellemo@sintef.no (L. Hellemo).

Received September 20, 2024; revised November 25, 2024; accepted December 20, 2024; available online January 3, 2025.

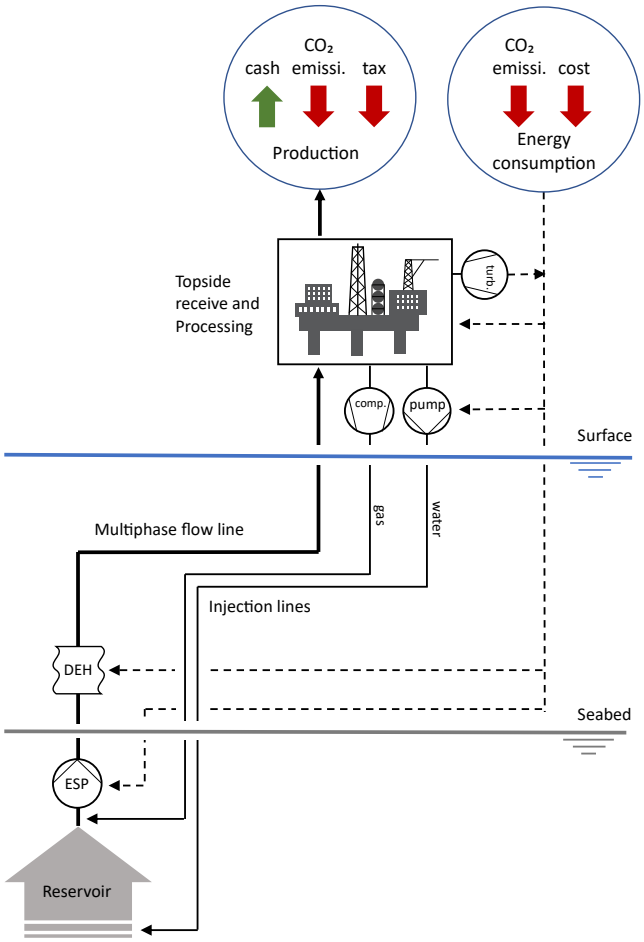

Fig. 1. Illustration of a hydrocarbon production system that takes into account the reservoir flow dynamics; the multi-phase well and flow lines that connect to first stage processing; process and down-hole production equipment, e.g., Direct electrical heating and Electrical submersible pumps, and finally production economy including production revenue, energy consumption and production, and emissions costs.

sion between the computational tools used for the daily production optimization and those used for long-term field planning optimization. Traditionally, production pipes and network simulations have been performed at time scales where reservoir responses can be approximated by simple inflow performance relations (IPR), while reservoir simulations were run largely ignoring dynamics above the reservoir. This is however no longer the case, and most industry grade reservoir simulators today support modelling of complex production networks where pressure drops along the network are modelled by vertical flow performance (VFP) tables generated from multi-phase pipe simulations. An open-source simulator that supports production network modelling is the *Open Porous Media (OPM) Initiative* OPM Flow (Rasmussen et al., 2021). Also, there have been several attempts at modelling reservoir responses beyond IPR for pipe and network simulation software, both for dynamic wellbore modelling (see e.g., da Silva and Jansen (2015) for a review) and for improved coupling (Guyaguler et al., 2011; Redick and Gildin, 2018; Hoffmann et al., 2019).

Both IPR-curves and VFP-tables serve as reduced order models for the well reservoir inflow and well flowline pipes, respectively. An IPR-curve is a simplified model for a well's phase or component flow rate as a function of its bottom-hole pressure (typically a good approximation only for a limited time-span). VFP-tables can be used as a computationally efficient replacement for a pipe/network simulator given that the occurring flow regimes are sufficiently sampled and sufficiently smooth. In the same manner, IPR-curves can be used as a computationally efficient replacement for the reservoir simulator but only on a time-span where the reservoir pressure remains more or less unchanged. In the following work detailed models are presented for the reservoir and well flowline network, connected through an implicit coupling. This setup is relatively computationally expensive, but it is shown that optimization still is practically possible. In future developments the aim is to add functionality for the creation of IPR and VFP models from the detailed modelling framework, that can be employed when greater optimization speed is desired.

Although there exist several commercial solutions for coupling of subsurface and surface facility simulation models, the authors are not aware of any existing fully open-source solutions that support fully implicit coupling strategies. It is however noted, that Chen (2020) considered an explicit coupling approach of MATLAB Reservoir Simulation Toolbox (MRST) to a surface network model using IPRs derived from *average* drainage regions. Although explicit couplings can be efficient in certain situations, the approach (Chen, 2020) was not successful in reducing oscillations for simulation cases using larger time steps. With the increased focus on carbon emissions, it becomes increasingly important to enable tighter and stronger coupling between the reservoir model, production network and surface facilities for improved long-term prediction modelling of multiple factors, such as production, economy, energy consumption and emissions. This work considers a coupling of MRST to an open-source multi-phase pipeline network simulator, with the intent to provide a research tool for studying integrated optimization. One advantage of employing MRST as the reservoir simulator is the availability of reduced order reservoir modelling tools (Lie and Krogstad, 2023, 2024) for exploring coupling strategies and speeding up optimization loops. The reduced order modelling approach also facilities uncertainty quantification and policy scenarios, because larger parameter spaces can be explored.

In addition to reservoir and multi-phase pipeline network coupling, the modelling framework presented in this work includes models for the initial separation and re-pressurization process, in terms of pump and compressor energy expenditure with regards to the oil, gas and water flow, including water/gas injection and export pipeline transport. In order to facilitate optimization in terms of profit and cost, a database of scenarios is compiled with current and future estimations of oil and gas prices, CO_2 taxes and electricity cost under uncertainty. An illustration of such a hydrocarbon production system is given in Fig. 1 for an offshore application.

In sum, this work presents a collection of open-source code intended for research on integrated field planning and

optimization. The code is located in a repository group on the SINTEF GitLab server, and the *Reservoir Network Coupling* repository in the group includes download and usage instructions. The paper proceeds as follows: first a description is given of the flow network modelling and a detailed description of the coupling strategies between the pipeline network and the reservoir model (for information on the reservoir model, MRST, see Lie (2019)). A description is then given of the integrated production optimization under uncertainty and market prices, energy cost and tax scenarios. Finally, three simulation examples are provided: A simplified example to illustrate coupling strategies (Section 4.1); reservoir-network coupling via a reduced model (Section 4.2); an optimization example with the full coupled system, including topside process and profit/cost scenarios (Section 4.3).

2. Flow network, reservoir modelling and coupling

This work considers the use and coupling of two distinct models, namely MRST for reservoir modelling and a flow network solver written in C++. The flow network solver is made accessible from MATLAB/MRST by a MEX-interface. All reservoir simulations are performed using the (automatic differentiation) AD-based solvers in MRST (Lie, 2019; Lie and Møyner, 2021), and coupling strategies heavily depend on the AD-generated Jacobians for the black-oil problems considered.

2.1 Flow network modelling

The network model is a one-dimensional steady-state model with a concept that is similar to the steady-state solvers in commercially available software like LedaFlow (Kongsberg Digital AS, 2024) or OLGA (SLB, 2024), solving for the mass flow rates and pressure in a network of pipes. The model works for any configuration of pipes, both converging (multiple pipes joining into one pipe) and diverging (one pipe splitting into multiple pipes) networks. The network model automatically discretizes each pipe into a number of cells, though the grid size can also be decided by the user. The default grid size is 20 D (D = pipe diameters) in vertical pipes and 40 D in horizontal pipes, with a linear weighting for inclinations between. In each cell the pressure drop and phase fractions are determined by a so-called Unit Cell Model (UCM), by using the mass flow rates and fluid properties as input. The UCM is a modelling concept commonly used in the oil and gas community. The UCM used in this study is based on the model described in Khaledi et al. (2014) and Smith et al. (2015), with several improvements implemented as part of the current work. The main improvements are:

1) The model has been extended to handle three-phase flow, though in a simplified manner. The oil and water are combined into a single liquid phase using mixture properties.
2) The robustness of the UCM has been significantly improved, both through an improved solution algorithm and by ensuring continuous and smooth physical models. The UCM is able to find a solution for all cases in an automated test set of 45 million simulations, covering a wide range of conditions.
3) The model has been rewritten from MATLAB to C++, making it significantly faster. Solving the model takes about 10^{-4} seconds on average (for the UCM, not the network model).

Just as for the previously published model, the UCM used in this study has some assumptions/limitations: (1) there is no slip between the entrained gas bubbles and the liquid, (2) there are no liquid droplets in the gas, (3) the oil and water are treated as a single liquid phase.

The UCM is a steady-state model, which means that it is valid for a single point in a pipe with constant flow rates, fluid properties and pipe properties. Such models are therefore also often referred to as "point-models". It should also be noted that though reasonable results can be expected, the predictions cannot be expected to be as accurate as using a commercial model, as this would require years of development. The UCM simply uses some commonly used closure laws found in the open literature, as is described in Smith et al. (2015). The inputs to the UCM are the mass flow rates ($\overrightarrow{mfr}$), fluid properties and pipe properties. From this the phase fractions ($\vec{\alpha}$) and pressure gradient ($(\mathrm{d}p/\mathrm{d}x)^{UCM}$) are calculated (Eq. (1)), and the pressure gradients in turn determine the pressure profile through Eq. (2):

$$UCM(\overrightarrow{mfr},\vec{\rho},\vec{\mu},\theta,D,\varepsilon) \longrightarrow \vec{\alpha}, \frac{\mathrm{d}p}{\mathrm{d}x}^{UCM} \tag{1}$$

where D is the pipe diameter, θ is the pipe inclination and ε is the pipe roughness, while $\vec{\rho}$ and $\vec{\mu}$ are the fluid densities and viscosities, respectively. To solve the pressure profile and phase fractions in an entire pipe or a network of pipes, the UCM needs to be solved in each cell coupled to each other. For a cell at index i:

$$p_{i+1} - p_i = \frac{\Delta x_i}{2}\frac{\mathrm{d}p}{\mathrm{d}x}_i^{UCM} + \frac{\Delta x_{i+1}}{2}\frac{\mathrm{d}p}{\mathrm{d}x}_{i+1}^{UCM} \tag{2}$$

Eq. (2) states that the difference in the pressure (p) between two neighbouring cells equals the pressure gradient given by the UCM (Eq. (1)) in the two cells, multiplied by half of each cell length (Δx). In addition, continuity is needed in the mass flow rates. The following equation relates the flow rate in and out of one cell to possible source terms (Γ) in the cell. The network solver has the ability to include both positive and negative mass sources at any location. If there are no sources, the flow rates in and out of the cell are equal:

$$\overrightarrow{mfr}_i^{out} - \overrightarrow{mfr}_i^{in} = \vec{\Gamma}_i \tag{3}$$

where both the mass flow rates and the source terms are in kg/s. Together Eqs. (2) and (3) give a coupled system matrix for all cells, with the mass flow rates and the pressure being the unknown variables. Note that the mass flow rates are stored at the cell faces, while the pressures are stored in the cell centres. The user can either specify constant fluid properties (though with a compressibility), or specify the path to a PVT-file with tabulated properties (generated with for instance PVTSim (Calsep, 2024) or Multiflash (KBC, 2024)).

Boundary conditions are also needed to close the system

of equations. The possible boundaries are:

1) Mass flow: Mass flow rates for all phases are specified.
2) Pressure: If there is flow from the pipe and into the pressure boundary, the pressure boundary only acts to connect the pressure in the pipe to a boundary pressure. If there is flow from the pressure boundary into the pipe, the boundary in addition acts to specify the flow rates (pressure driven flow rates).
3) Junction: The boundary can also be a junction, which acts similarly to a pressure boundary, with either inflow or outflow. In addition, an extra set of equations is available for conservation of the mass flow rates through the junction.

The network model also has some assumptions and limitations:

1) There is no phase change (evaporation or condensation).
2) For diverging networks, a simplifying assumption is made that the flow split through a junction is the same for all phases. For the scenarios presented in this study however, only converging networks are used.
3) There are no temperature calculations, so the temperature must be given by the user. A single temperature can be given for the entire pipe, or the temperature can be individually specified for different parts of the pipe, or even for each cell. This allows for specifying a non-uniform temperature profile along the pipe, if one has an approximate idea of what that temperature profile would be.

2.2 Model coupling

Coupling of distinctly different simulation models is a common but challenging task, particularly for different time-dynamics. For reservoir simulations typically requiring a fully implicit solution procedure for stability, it is not likely that any form of explicit coupling to a network model (with even faster dynamics) will be successful. Accordingly, the aim is a fully implicit solution of the coupled network-reservoir system.

For a detailed description of the discretized equations describing a three-phase black-oil model, the reader is referred to Lie (2019) and Lie and Møyner (2021). Herein, we will simply denote as $\boldsymbol{x}_{r,k}$ the vector of all unknown primary variables at simulation step k. Hence, $\boldsymbol{x}_{r,k}$ contains pressures and phase saturations for every grid cell in addition to bottom-hole pressures and rates for each well. In the fully implicit approach, each simulation time step involves solving a nonlinear system of equations:

$$r_r(\boldsymbol{x}_{r,k}, \boldsymbol{x}_{r,k-1}) = \boldsymbol{0} \tag{4}$$

where $\boldsymbol{x}_{r,k-1}$ contains the (*known*) primary variables of the previous step, and all property evaluations in r_r depend on the *unknown* $\boldsymbol{x}_{r,k}$. The system in Eq. (4) is solved to a given tolerance by the Newton-Raphson method, where the i^{th} iteration update $\delta\boldsymbol{x}_{r,k}^{(i)}$ is obtained by solving the linear system:

$$J_{r,k}^{(i-1)} \delta\boldsymbol{x}_{r,k}^{(i)} = -r_r(\boldsymbol{x}_{r,k}^{(i-1)}, \boldsymbol{x}_{r,k-1}) \tag{5}$$

where $J_{r,k}^{(i-1)} = \partial r_r \left(\boldsymbol{x}_{r,k}^{(i-1)}, \boldsymbol{x}_{r,k-1}\right) / \partial \boldsymbol{x}_{r,k}^{(i-1)}$ is the Jacobian matrix of all partial derivatives. As previously mentioned, the Jacobian of the reservoir equations is generated by automatic differentiation (Lie and Møyner, 2021).

For a given time step k, consider the discrete reservoir system of equations $r_r(\boldsymbol{x}_{r,k}, \boldsymbol{x}_{r,k-1}) = \boldsymbol{0}$, and the steady-state discrete network system of equations $r_n(\boldsymbol{x}_n) = \boldsymbol{0}$. For the two systems to be compatible, there are (assuming a three-phase system) four quantities per well that need to match between the two systems. These are the three-component mass flow rates (or volume rates at specified conditions) and the bottom-hole pressure (bhp). These correspond to each well's primary variables in MRST (assuming the standard well model is used), and likewise, to the primary variables for the network solver in its boundary node.

Accordingly, the two systems may be rephrased as:

$$r_r(\boldsymbol{x}_{r,k}, \boldsymbol{x}_{r,k-1}, \boldsymbol{x}_{n,k}) = \boldsymbol{0} \text{ and } r_n(\boldsymbol{x}_{r,k}, \boldsymbol{x}_{n,k}) = \boldsymbol{0} \tag{6}$$

where e.g., r_r sets up its well control equations as bhp-control with values taken from the corresponding network solution node pressures, and r_n sets up its corresponding boundary conditions with mass rates taken from the reservoir solution. In a fully implicit coupling strategy, analogously to Eq. (5), a Newton update of the coupled system becomes:

$$\begin{pmatrix} \boldsymbol{J}_{rr} & \boldsymbol{J}_{rn} \\ \boldsymbol{J}_{nr} & \boldsymbol{J}_{nn} \end{pmatrix} \begin{pmatrix} \delta\boldsymbol{x}_r \\ \delta\boldsymbol{x}_n \end{pmatrix} = \begin{pmatrix} -\boldsymbol{r}_r \\ -\boldsymbol{r}_n \end{pmatrix} \tag{7}$$

where $J_{ij} = \partial r_i(\boldsymbol{x}_i) / \partial \boldsymbol{x}_j$ and where the k step index and (i) iteration index have been omitted for brevity. In essence, there is no difference between Eqs. (5) and (7). In practice, however, if the two models are implemented in separate simulators, constructing the coupled system Jacobian matrix Eq. (7) can be challenging. For the code presented herein, the implicit coupling is performed using the AD-functionality of MRST and equipping the network solver with functionality to output its Jacobian matrix. Hence for a given Newton update, $\boldsymbol{J}_{rr}$ and $\boldsymbol{J}_{nn}$ are available, so the missing pieces are the Jacobian *cross terms* $\boldsymbol{J}_{rn}$ and $\boldsymbol{J}_{nr}$. In this implementation, the coupling matrix $\boldsymbol{J}_{rn}$ picks out the boundary node pressure updates for the network model to enforce continuity in pressure, while $\boldsymbol{J}_{nr}$ picks well component rate updates from the reservoir model to enforce flux continuity. It is noted that this merging only takes effect for the production networks, as the simplifying assumptions have been made that injection networks only consist of single pipes with flow rate control without pressure limits. In this way injector bhps can be determined solely based on the reservoir model, and the coupling becomes *one-way*.

Three solution strategies have been implemented for the coupled system of Eq. (6) that all (if successful) converge to fully implicit solutions of the coupled system. The first, however, uses a simple *fixed-point* strategy where forming the coupled Jacobian matrix is not required.

(1) *Sequentially fully implicit* (SFI). This is the least intrusive approach, and simply alternately solves the two systems until converged. One outer iteration of this approach is achieved

by first solving the (non-linear) reservoir equations with fixed bhps obtained from the previous network solver boundary node pressure values, and then solving the (non-linear) network equations with boundary node mass rates obtained from the previous reservoir solution. Accordingly, at iteration i, the solution sequence is:

$$r_r(\boldsymbol{x}_r^{(i)}, \boldsymbol{x}_n^{(i-1)}) = \mathbf{0}$$
$$r_n(\boldsymbol{x}_r^{(i)}, \boldsymbol{x}_n^{(i)}) = \mathbf{0}$$

In effect, this a fixed-point approach where one cannot hope for more than linear convergence. Compared to the standard fully implicit approach, this potentially is a computationally costly approach, since in each coupled non-linear iteration, it needs to solve both the non-linear reservoir and network systems (and not just a linearized system). Also, for more complex systems, convergence can be hard to obtain at all.

(2) *Fully implicit* (FI). For the standard fully implicit approach, the equations are solved fully coupled as Eq. (7). In the examples presented herein, the coupled linear systems are solved using a direct sparse method (MATLAB's *backslash*) which is not efficient for problems exceeding $\approx 10^6$ unknowns. In a more unified framework, it is expected that a tailored constrained-pressure-residual (CPR) approach would be the best option for solving linear systems on the form Eq. (7).

(3)*Fully implicit with local network solves* (FI-LNS). If the non-linear dynamics in the network is much faster than in the reservoir, it can be advantageous to spend extra iterations on the network solver, in order to reduce the number of global Newton iterations. In this third option, the full non-linear network equations are solved keeping the current reservoir states fixed, in between each coupled Newton iteration. Hence, before each coupled Newton iteration i, the procedure is to solve $r_n(\boldsymbol{x}_r^{(i-1)}, \boldsymbol{x}_n^{(i-\frac{1}{2})}) = \mathbf{0}$ with $\boldsymbol{x}_r^{(i-1)}$ fixed. Note that this yields $\boldsymbol{r}_n \approx \mathbf{0}$ for the subsequent coupled iteration Eq. (7)).

Section 4.1 presents a simple comparison of the three coupling approaches.

3. Integrated production optimization

Integrated production optimization is a discipline that considers both long-term and short-term timescales when optimizing field operation decisions. A physics-based integrated model of reservoir and production network facilities could provide more realistic forecasts for production planning than standalone models. An important aspect of integrated modelling is how the coupling between the reservoir and gathering network works, with different approaches described in Section 2.2.

When it comes to the optimization of an integrated model, different approaches can be used, depending on the characteristics of the models, the timescale of the decisions and the overall goals. Traditionally, in well control optimization problems, response surfaces can be regarded as having a smooth curvature. In such cases, there are simulators that implement adjoints and provide sensitivities with respect to the control variables, allowing the use of gradient-based methods (Brouwer and Jansen, 2004; Sarma et al., 2006; Kraaijevanger et al., 2007; Bukshtynov et al., 2015). Even though MRST has flexible adjoint capabilities, this has not been carried over to the coupled reservoir-network solver, so in the coupled setting adjoints are currently not an option. It is however noted that gradient-based optimization may not be the best option if problems are not sufficiently smooth. In practical applications, adjoint-based gradients may also be sensitive to simulator adaptive time-stepping and accuracy (tolerance) of the forward solver.

While gradient-based approaches can be efficient if derivatives are trusted (Jansen, 2011), derivative-free methods are often a practical alternative when gradients are unavailable, or are unreliable due to cost function discontinuities caused by simulation-based constraints. Compared to gradient-based methods, derivative-free approaches tend to require a larger computational budget for optimization, mainly due to the lack of the additional information provided by the approximation model when evaluating new candidate solutions during the optimization search (Ciaurri et al., 2011).

3.1 Production optimization under uncertainty

The objective function adopted is an economic measure that incorporates key financial parameters, such as oil and gas prices and the costs associated with water injection and emission costs. Specifically, the objective function is the Net Present Value (NPV), which is calculated from a series of cash flows over a specified time period. The NPV may be expressed as:

$$\mathrm{NPV}(\mathbf{q}_\mathrm{u}) = \sum_{t=1}^{T} \frac{1}{(1+d)^{\hat{\tau}(t)}} \left[\hat{r}_\mathrm{og}(\mathbf{q}_\mathrm{u}, t) + \hat{r}_\mathrm{gg}(\mathbf{q}_\mathrm{u}, t) - \hat{r}_\mathrm{pc}(\mathbf{q}_\mathrm{u}, t) - \hat{r}_\mathrm{ec}(\mathbf{q}_\mathrm{u}, t)\right] \tag{8}$$

with $\mathbf{q}_\mathrm{u}$ being a vector with the rates of gas, oil and water rates for all time steps $t = 1, \ldots, T$. For given flows $\mathbf{q}_\mathrm{u}$ at time t, the gains/costs are given by the following functions: $\hat{r}_\mathrm{og}(\cdot)$ for oil production gains; $\hat{r}_{gg}(\cdot)$ for gas production gains; $r_\mathrm{pc}(\cdot)$ for the topside process costs; and $r_\mathrm{ec}(\cdot)$ the CO_2 for the emission costs. The function $\hat{\tau}(t)$ maps the current time t to the corresponding year of production. The revenue generated from field production is discounted over time using a discount factor d.

An ensemble of reservoir models represents the geological uncertainty present in the models. For this reason, instead of maximizing the NPV of a single realization, the objective function is the expected value of the NPV for the ensemble. As all the realizations which belong to the ensemble are considered equally probable, the expected value is given as the mean of the NPV values computed across all realizations, namely:

$$f(\mathbf{q}_\mathrm{u}) = \frac{1}{M} \sum_{i=1}^{M} \mathrm{NPV}_i(\mathbf{q}_\mathrm{u}) \tag{9}$$

in which $\mathrm{NPV}_i(\mathbf{q}_\mathrm{u})$ is the economic function resulting from the i^{th} realization, assuming a well control sequence $\mathbf{u}$, and M is the number of reservoir realizations.

The production optimization problem for an ensemble of geological realizations can then be formulated as:

$$P: \underset{\mathbf{u}}{\text{maximize}} \quad f(\mathbf{q}_u) \tag{10a}$$

subject to:

$$R_i(\mathbf{x}_0, \mathbf{x}_u, \mathbf{u}) = 0, \qquad \forall i = 1, \ldots, M \tag{10b}$$

$$\mathbf{q}_u = Q(\mathbf{x}_u) \tag{10c}$$

$$\mathbf{u}_{lb} \leq \mathbf{u} \leq \mathbf{u}_{ub} \tag{10d}$$

$$\mathbf{c}(\mathbf{u}) \geq 0 \tag{10e}$$

The reservoir and network equations of the integrated model for each ensemble member i are denoted by $R_i(\mathbf{x}_0, \mathbf{x}_u, \mathbf{u})$ in Eq. (10b), where the reservoir states are $\mathbf{x}_u$, and the well controls are $\mathbf{u}$.

The initial states are given by $\mathbf{x}_0$, and the control sequence and corresponding flow rates are computed from the states using $Q(\mathbf{x}_u)$ in Eq. (10c). The constraints Eqs. (10d) and (10e) are bounds on the well controls and some additional inequality constraints, respectively. The lower and upper bounds $\mathbf{u}_{lb}$ and $\mathbf{u}_{ub}$ are typically used to impose physical or user-set limits that prevent invalid control strategies, such as too low pressures (causing production issues), or too high pressure for injectors, exceeding formation or equipment limits. Inequality constraints Eq. (10e) on the input variables $\mathbf{u}$ are used to limit the field-wide production on the platform, such as the total water handling limits or environmental constraints.

3.2 Derivative-free trust region optimization

Among the available derivative-free optimization methods, model-building approaches tend to present a better convergence performance and require less computational budget than model-free or pattern-search approaches. This is mainly because the model-building methods rely on the construction of a model (polynomials, Gaussian distributions, and linear regression) that provides additional information during the optimization search. Derivative-free trust region methods have exhibited good performance in production optimization problems, particularly because of their ability to reach close-to-optimal solutions with fewer function evaluations than model-free approaches (Conn et al., 2000, 2009).

A derivative-free trust region algorithm is applied for the optimization of the robust well control problem. The method constructs a polynomial interpolation model using simulated data points, providing a locally valid approximation of the underlying cost function. The next candidate solution is determined by minimizing this approximate model. Compared to direct-search sampling methods, the inference of curvature information through the approximate model is expected to enhance the efficiency of the search within the feasible space. The model-building process of the derivative-free trust region method relies on a polynomial interpolation of objective function values, which in the robust well control problem will be the expected NPV for all the realizations. The subsequent search for new tentative solutions relying on this interpolation is regarded as less sensitive to objective function noise and error.

More information about the derivative-free algorithm used in this example, with implementation details and applications to production optimization can be found in Silva et al. (2020) for deterministic problems, and more thoroughly reported in Silva et al. (2022) for production optimization problems under uncertainty. Recent studies, as reported in Hannanu et al. (2024a, 2024b), proposed extensions to the derivative-free trust region optimization algorithm to account for output constraint-handling in the presence of uncertainty.

3.3 Market prices and scenarios

Commodity prices are crucial parameters in optimizing profitability of petroleum production. To facilitate access and use of price estimates gathered from multiple sources, a software package is developed to simplify versioned access to datasets for easy reproduction and documentation of assumptions, as not all sources include all commodities. For transparency the raw results from different studies have been included in the package in addition to adapted prices. The analyses require both short- and long-term estimates, and the prices with estimates of uncertainty have been gathered from multiple sources before being made available in a common format.

For short-term estimates, historical data is used for electricity prices, wind and PV production, oil and gas prices, and CO_2 emissions. For long-term projections, estimates are obtained from openly available research reports. For oil and gas prices, the long-term values are based on the International Energy Agency's various future scenarios, including the Net-Zero-Emissions by 2050 scenario, which predicts low oil prices (USD 24/barrel) and high CO_2 prices (USD 250/tonne) (Bouckaert et al., 2021).

For electricity price scenarios, data is more variable and dependent on numerous factors like technology costs, demand, energy mix, and policies. Studies from the Norwegian TSO Statnett (Statnett, 2020) and The Norwegian Water Resources and Energy Directorate (Jelsness, 2020) provide some future projections for electricity prices for Norway and Europe.

The software package is designed to allow for flexible scenario creation defined by parameters such as the market scenario, reference years, and methodologies, ensuring consistency and provenance of data. The resulting market data for the analyses below are represented as three generic price scenarios: -Low, Medium, and High-.

4. Numerical examples

Three numerical experiments will now be presented with increasing complexity to illustrate usage of the software. A simplified example to illustrate coupling strategies. A reservoir-network coupling via a reduced modelling of the flow in the reservoir. And, finally, an optimization example with the full, coupled system, including topside process and profit/cost scenarios.

4.1 A simple example for testing coupling strategies

As a simple illustrative example comparing coupling strategies, a modified version is considered of the SPE1 model (Odeh, 1981). This is originally a small black-oil model with a single injector and producer. In this setup, the injector is re-

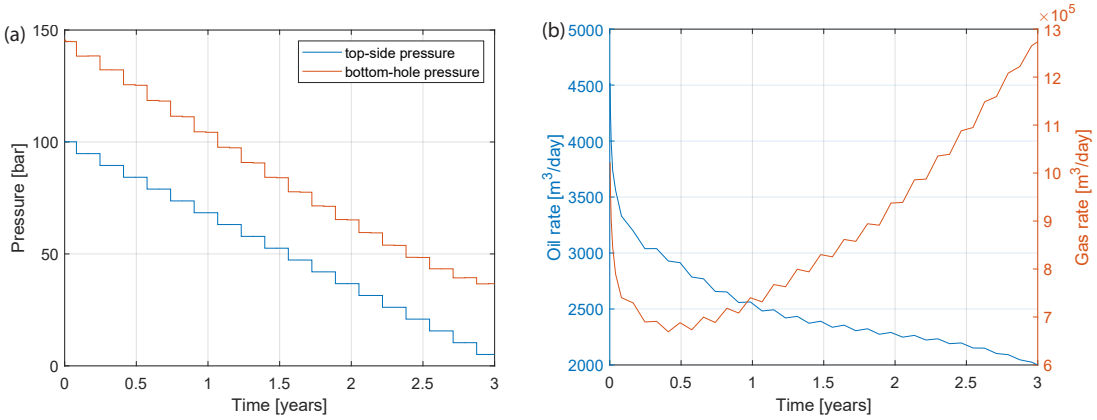

Fig. 2. Simulation results for the example based on the SPE1-test. (a) Left plot shows topside pressure (control input) and bhp for producer and (b) right plot shows oil/gas production rates at surface conditions.

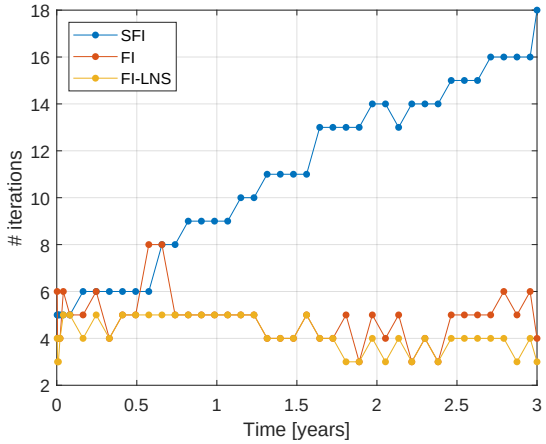

Fig. 3. Outer iteration counts per time step for the three coupling strategies SFI, FI and FI-LNS.

moved (i.e., no pressure support), and a 1,000 meters long vertical pipe is attached to the producer. The producer is controlled by its topside pressure which at the beginning of the simulation is set to 100 bar, but then reduced every 60 days until the end of simulation, when it is at 5 bar. Since there is no pressure support, the reservoir pressure drops substantially during this simulation.

Fig. 2(a) reports the topside pressure (the control) and corresponding bhp for the producer. The pressure drop in the pipe (difference between the two), is mainly due to gravity and friction. Initially there is no free gas in the reservoir, but as pressure drops below the bubble point in the reservoir, gas production increases (right plot). The effect of increasing gas-to-oil ratio on pressure drop in the pipe, is initially a decrease due to less dense mixture. However, toward the end, an increase can be observed due to the high gas flow rate such that friction and acceleration accounts for more than 25% of the total pressure drop.

Fig. 3 reports the number of *outer* iterations required for each time step for each of the three strategies. Note that a single iteration for the sequential strategy is much more computationally expensive than the other two approaches, since it solves both non-linear systems to convergence. The least costly iteration is naturally the standard fully implicit strategy since this amounts to just solving the coupled linear system. It is clear from Fig. 3 that the increased gas-to-oil ratio makes the coupled problem harder for the sequential strategy to solve, even for this simple problem setup, so it is not advisable to use this approach for more complex problems. As expected, the FI-LNS requires slightly less iterations than the FI, but it is also slightly more expensive, so for this example, their performances are more or less equal. We have observed, however, that the FI-LNS is the most robust option, so for the remaining numerical examples this will be the preferred strategy.

4.2 Reservoir-network coupling via a reduced model

In this example a detailed reservoir simulation model is coupled to the pipe network model via a *proxy* that is continuously calibrated to output from the detailed model. In this way, the implicit coupling between reservoir and network is still used, but the detailed reservoir simulation is considered *black box* (and could in principle have been performed using any simulator).

The example model is an altered version of an MRST test-case which is based on the Norne field grid model. It is however slightly altered to better serve the purpose of illustrating the coupling methodology. It is noted that this is a two-phase oil/water model, which results in a less challenging simulation of the flow in pipes. On the other hand, low compressibility, and hence fast reservoir pressure propagation, makes the coupling more challenging (and global). Fig. 4(a) shows the Norne model and the wells used for this example. For the simulation schedule, the following is defined:

(1) The six injection wells all inject water at a constant rate of 1,296 m^3/day.

(2) The three producer wells P1, P2, P3 are connected to inclining pipes of lengths 500, 750 and 600 m, respectively, that all meet in a manifold. From the manifold there is a vertical riser of length 500 m and at the top a pressure boundary condition of 10 bar is imposed.

(3) The simulation is run for 40 years with time steps of 30 days.

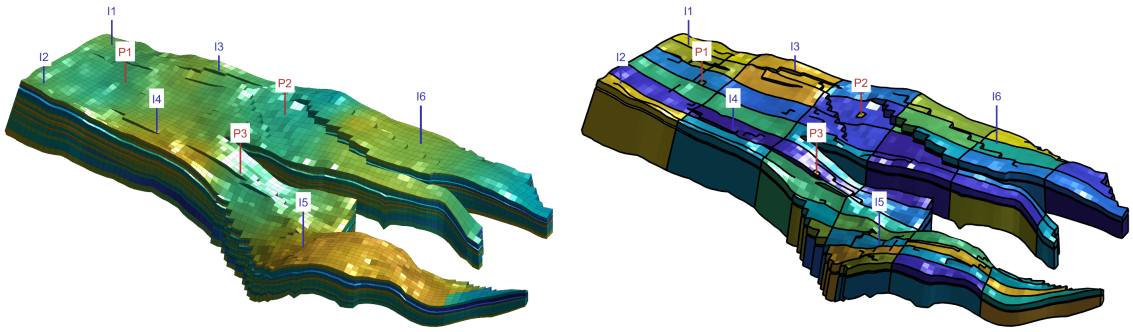

(a) (b)

Fig. 4. (a) Norne model and considered wells where cells are coloured by the logarithm of the horizontal permeability and (b) the right plot depicts partitioning into coarse blocks used for the coarse models.

Reduced reservoir modelling. The purpose of this example is to illustrate how the network coupling can be solved with a reduced order reservoir model that *shadows* the (local in time) response of the detailed reservoir model. There are many possible candidates for such a reduced order model, but here the MRST-functionality for coarse grid network models (Lie and Krogstad, 2023, 2024) is utilized. In this approach the detailed reservoir grid is partitioned into very coarse blocks that serve as basis for a very coarse reservoir model. The petrophysical parameters of this model are then considered free and are calibrated so that model output matches that of the detailed model. Parameter sensitivities are obtained by adjoint simulations and calibration/optimization is performed using the Levenberg-Marquardt algorithm.

Coarse model generation is based on a $[10, 6, 1]$ logical partitioning of the 44,915 cells in the detailed model grid. In addition, since high accuracy is desired, the detailed grid well cells are included as separate blocks in the coarse partitioning, in order to have sufficient *parameter-resolution* around wells. The resulting coarse partitioning is depicted in Fig. 4(b). Due to an impermeable layer in the model, most of the coarse blocks have been split horizontally, since the coarsening algorithm assures that all coarse blocks are connected. In effect, the resulting coarse model can be considered a two-layer model. For calibration, an objective function is used that calculates a mismatch value according to:

$$J = \sum_{m=1}^{N_w} \sum_{k=1}^{N_t} \frac{\Delta t_k}{\mathscr{T}} \left(\frac{e_{k,bhp}^2}{w_{bhp}^2} + \frac{e_{k,w}^2}{w_w^2} + \frac{e_{k,o}^2}{w_o^2} \right) \tag{11}$$

in this expression, N_w is the number of wells, N_t is the number of time steps and $\mathscr{T}$ is the total simulation time. Furthermore, $e_{k,bhp}$, $e_{k,w}$ and $e_{k,o}$ denote the respective mismatches in bhp, water-rate and oil-rate for time step k. Finally, the w_{bhp}, w_w and w_o are weights that are set according to the magnitude of pressure variances and flow rates for the model under consideration. In this example, $w_{bhp} = 100$ bar and $w_w = w_o = 1{,}000$ m^3/day is used, and the aim is a mismatch $J < 10^{-5}$.

Coupled simulation strategy. The simulation is divided into *episodes* where in each episode the aim is to have a reduced reservoir model that sufficiently matches the fine model, and where the episode can be re-run whenever the reduced reservoir model needs re-calibration. Let $\boldsymbol{x}_{r,k}$ and $\boldsymbol{x}_{rc,k}$ denote the fine model and coarse model reservoir states at time step k, and let $\boldsymbol{x}_{p,k}$ denote the corresponding pipe/network states. For ease of notation, consider simulating the coupled system from time zero to ΔT by performing m time steps. That is, it is desirable to obtain $\boldsymbol{x}_{r,1:m}$ and $\boldsymbol{x}_{p,1:m}$. This involves the following steps:

(1) Simulate the coupled proxy-network model with the imposed topside boundary condition for m time steps to obtain states $\boldsymbol{x}_{rc,1:m}^{(i)}$ and $\boldsymbol{x}_{p,1:m}^{(i)}$.

(2) Simulate the fine reservoir model for m time steps using well controls (bhps) $\boldsymbol{u}_{rc,1:m}^{(i)}$ fetched from $\boldsymbol{x}_{rc,1:m}^{(i)}$ to obtain $\boldsymbol{x}_{r,1:m}^{(i)}$.

(3) Fetch coarse model well output (bhps and rates) $\boldsymbol{y}_{rc,1:m}^{(i)}$ from $\boldsymbol{x}_{rc,1:m}^{(i)}$ and fine model well output $\boldsymbol{y}_{r,1:m}^{(i)}$ from $\boldsymbol{x}_{r,1:m}^{(i)}$. Then if

$\|\boldsymbol{y}_{r,1:m}^{(i)} - \boldsymbol{y}_{rc,1:m}^{(i)}\| \leq \text{tol}$:

Set $\boldsymbol{x}_{r,1:m} = \boldsymbol{x}_{r,1:m}^{(i)}$, $\boldsymbol{x}_{p,1:m} = \boldsymbol{x}_{p,1:m}^{(i)}$ and return.

$\|\boldsymbol{y}_{r,1:m}^{(i)} - \boldsymbol{y}_{rc,1:m}^{(i)}\| > \text{tol}$:

Re-calibrate coarse model to match $\boldsymbol{y}_{r,1:m}^{(i)}$,

set $i = i + 1$ and go to Step 1.

It is noted that an initial coarse model is needed for the first episode, and for the current example this is obtained by running the fine reservoir model for a few time steps and training the initial coarse model to match these. The re-calibration of the coarse model can be performed on any amount of past *history* from the fine reservoir model. For illustration, we consider the following combinations of episode lengths versus re-calibration history.

(1) 6-month episodes/6 previous months re-calibration.

(2) 1-month episodes/4 previous months re-calibration.

In the first case, six month episodes are chosen and utilize fine model output from the current episode whenever re-calibration is needed. Hence, the coarse model is updated at most every six months. For the second case shorter episodes are used (one month) but re-calibration is performed over the last four episodes. For both cases the mismatch tolerance is

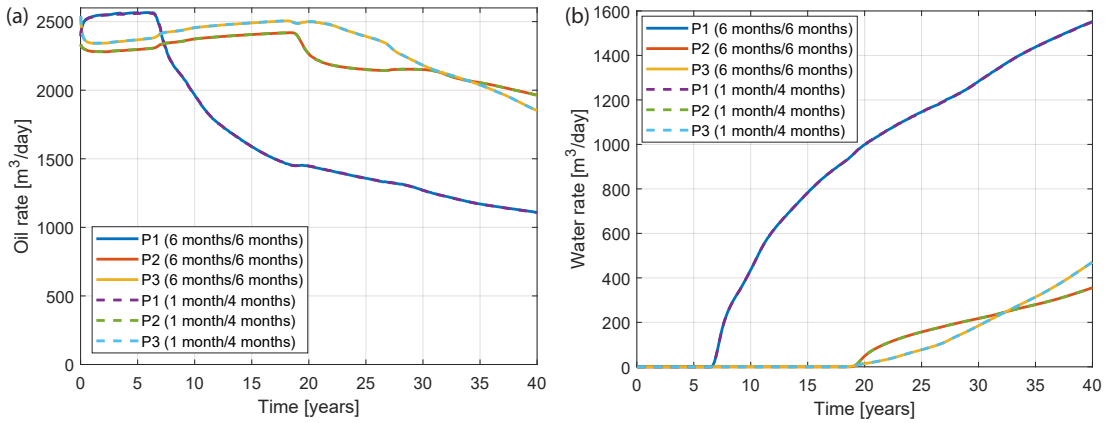

Fig. 5. (a) Oil and (b) water production rates for the Norne example obtained with the two simulation cases using 6-month episodes/6-month re-training (solid lines) and 1-month episodes/4-month re-training (dashed lines). Note that curves for the two cases are overlapping.

set to tol $= 10^{-5}$, which is sufficiently strict that that well curves completely overlap in *eye-norm* for the fine and coarse model. As seen in Fig. 5, this also holds true for the two coupled cases. For both cases a single re-calibration is required for most episodes although a few don't need calibration at all. At the water breakthrough of well P1, two re-calibrations are needed to reach the desired agreement between the fine and coarse models. For the current implementation the case with 6-month episodes/6-months re-training is the most computationally efficient, since the model re-calibration is much more frequent in the case using 1-month episodes/4-months re-calibration. This is however in part due to the significant relative overhead of running small models in MRST. In terms of fine model evaluations, the two cases are fairly equal (in complexity approximately equal to two *uncoupled* full reservoir simulations).

4.3 Optimization example

A production optimization example will now be explored of the integrated model with multiple geological realizations of a detailed reservoir simulation model, coupled to a steady-state gathering network model and topside facilities. The objective function is the NPV for a selected market scenario that includes the revenue from selling of the produced oil and gas, subtracted by operational costs such as water handling and energy costs. Optimization is performed considering a time span of 4 years, with two control variables per well, the topside pressure for the production wells, and the water or gas flow rates for the injection wells.

The optimization example considered is an instance of the problem formulated in Eqs. (10a)-(10e), also discussed in Section 3.1. The example uses the synthetic *Egg* reservoir as given by Jansen et al. (2014). The original model is two-phase oil/water, that has been extended to a three-phase black-oil model to enable more dynamic pipe flow. The reservoir is positioned 600 m from the ocean surface, with production and injection flow lines extending from a topside processing facility on a surface rig down to the reservoir. The following setup for the simulation is used:

(1) There are 8 injection wells, where 4 inject water and 4 inject gas, as given in Fig. 9.

(2) The 4 production wells are connected to production multi-phase flow lines. The flow lines have pipe segment lengths 200, 96, 267, 103, 220 and 50 m, having the respective angles (relative to the horizontal) 90, 0, 50, -29, 85, and 0 degrees, as illustrated in Fig. 9. The production wells have a diameter of 41 mm, and a constant temperature of 50 degrees Celsius is to all flow lines pipeline segments.

(3) A topside process with 3 stage separation and 4 stage compressor re-pressurization for gas injection and export, as given in Fig. 8, where P_1 is the topside pressure after the choke, and P_2 and P_3, are set to 10 and 1.5 bar, respectively. The mass fractions of gas passing compressors 2 and 3 are set to 0.07 and 0.01, respectively. Therefore, the separation of gas from liquid is not modelled as dependent on flow rates in the topside process system. Oil and water separation is considered to be 100%, hence cost for water treatment is not considered in the current case. Pumps for oil export and water injection are included, and relevant pump and compressor curves are used to calculate the energy expenditure of the topside process (Schümann and Bergmo, 2022).

(4) The simulation is run for 4 years. The first five time steps have a duration of 0.1, 0.9, 4, 10 and 15 days, and subsequent time steps have a duration of of 30 days.

For this example, 5 geological realizations are chosen for the reservoir model, as depicted in Fig. 6, with the producers coupled to a gathering network.

As the Egg model is a channelized reservoir, the geological uncertainty is represented with different patterns for the high permeability channels (realizations 1 to 5 from top-left to bottom-right). In this way, a control strategy will have different production performance, and thus different NPV values, for each realization. The defined optimization problem will maximize the expected NPV value, which in this case is the mean NPV, as all the realizations are considered equally probable.

As for the market scenarios, as described in Section 3.3, the uncertain parameters are electricity prices, natural gas prices,

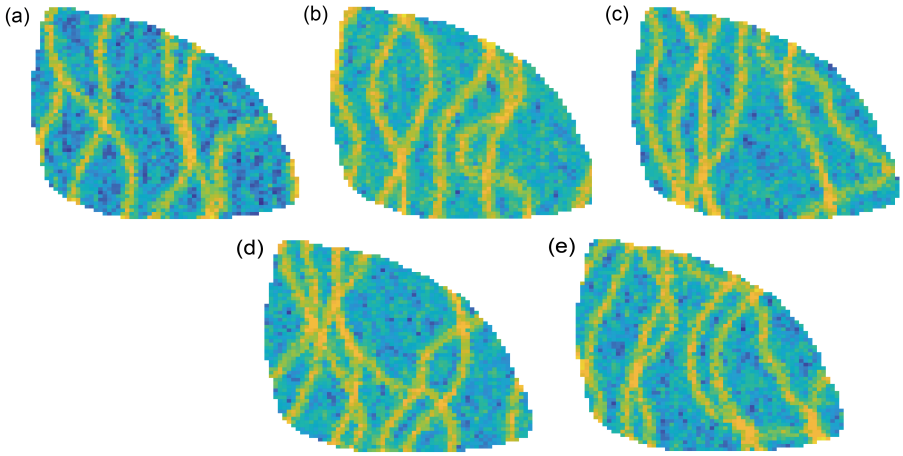

Fig. 6. Log-permeabilities of three-phase Egg model realizations 1 to 5, given in subfigures (a) to (e).

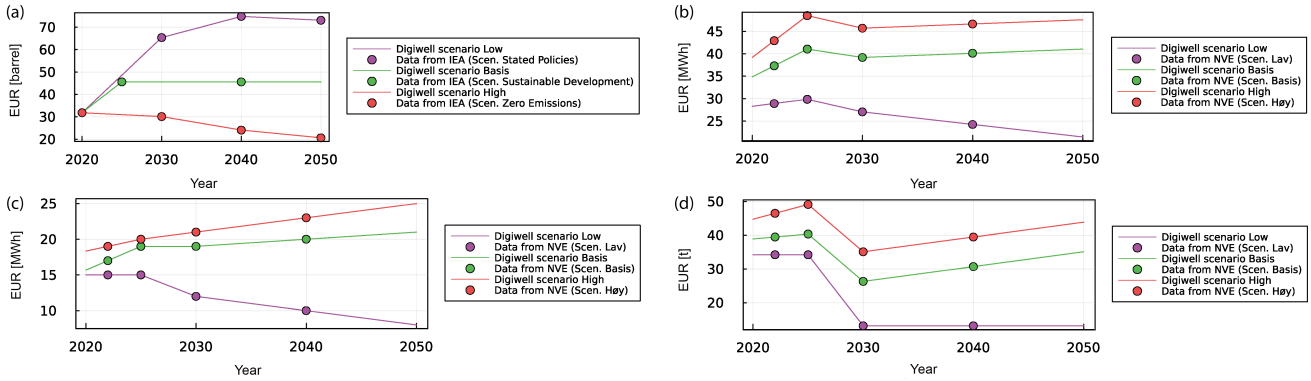

Fig. 7. Market scenarios Lav, Basis, Høy (Low, Base, High) for the prices (from Jelsness (2020)) and (Zero Emissions, Delayed Recovery, Stated policies) for the oil price (from Bouckaert et al. (2021)). The selected scenario used in the optimization example include (a) low crude oil price, (b) low electricity price, (c) low natural gas price and (d) Zero Emissions scenario, high tax on CO_2.

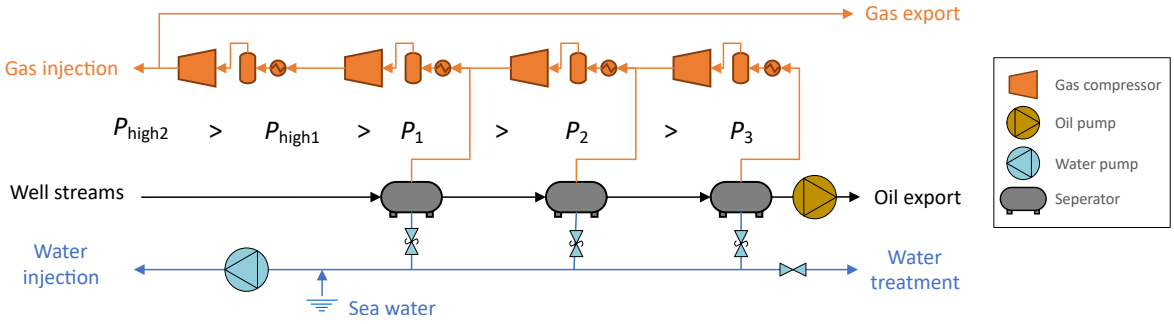

Fig. 8. Topside process (illustration from Schümann and Bergmo (2022), modified with permission) with 3 stage separation and 4 stage compressor re-pressurization for gas injection and export. Here, P_1 is the topside pressure after the choke, and P_2 and P_3, are set to 10 and 1.5 bar, respectively. The mass fractions of gas passing compressors 2 and 3 are set to 0.07 and 0.01, respectively. Pumps for oil export and water injection are included, and relevant pump and compressor curves are used to calculate the energy expenditure.

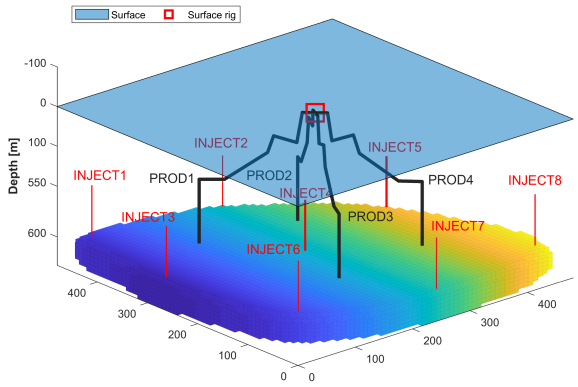

Fig. 9. The synthetic reservoir case *Egg* as given by Jansen et al. (2014). There are 8 injection wells, where 4 inject water and 4 inject gas. There are 4 production flow lines (shown as grey lines), that connect to a topside process shown in Fig. 8.

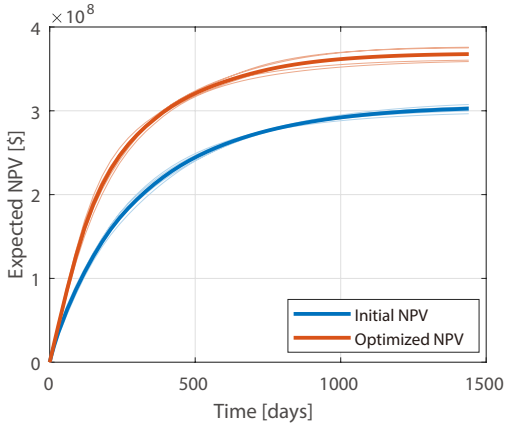

Fig. 10. Evolution of expected NPV for the initial and optimal controls (thick lines). Thin lines show evolution for individual ensemble members.

crude oil prices and the CO_2 tax associated with natural gas and crude oil production. Categories used for the oil prices are 'Zero Emissions', 'Delayed Recovery' and 'Stated policies' (Bouckaert et al., 2021). The other parameters have the categories 'Low', 'Base' and 'High' (Jelsness, 2020). This example uses a scenario with low electricity price, low natural gas price, zero emissions scenario (high tax on CO_2), and low crude oil price, as given in Fig. 7.

The initial controls ($\mathbf{u}_0$) provided to the optimization are:

(1) Water injection rate (surface conditions), q_w = 259 m^3/day.

(2) Gas injection (surface conditions), q_g = 25,920 m^3/day.

(3) Producers topside pressure, p^{sep} = 240 bar.

Lower and upper bounds for the injectors mass flows and topside pressure for the producers are set as constraints in the optimization:

(1) Water injection bounds, 86 m^3/day$\leq q_w \leq$501 m^3/day.

(2) Gas injection bounds, 8,640 m^3/day$\leq q_g \leq$40,000 m^3/day.

(3) Producers topside pressure bounds, 220 bar $\leq p^{sep} \leq$ 280 bar.

The objective function is the expected NPV for all the geological realizations calculated from the resulting well flows obtained with the controls $\mathbf{u}$.

The algorithm supports different types of constraints on the control variables: Bound constraints, linear equality constraints and linear inequality constraints. For this example, however, only bound constraints are used. Standard stopping criteria are the minimum step length or radius size. Since each linear system of the coupled model is solved using a direct sparse solver, the simulation of a single realization takes approximately 20 minutes. Accordingly, since ensemble simulations are run in parallel this is also the evaluation time of one function evaluation during optimization. The trust region algorithm is run for 50 iterations (124 function evaluations).

The NPV evolution for the initial and optimized control settings are shown in Fig. 10. Increased expected NPV is observed over the initial controls for the optimized solution. Furthermore, a slightly larger spread (thin lines) is seen among the realizations for the optimized solution compared to the initial. Fig. 11 depicts the optimized controls for the gas injectors (left), water injectors (middle) and producers (right). For all gas injectors, It is observed that the suggested strategy is to inject at full capacity for the first period while reducing to the minimal for the second. All water injectors are suggested to inject at full capacity for the entire time horizon. For the producers, the situation is a bit less uniform, and indicates that PROD1 is the most profitable well (operating at its minimum pressure) while PROD3 is operating at its maximal pressure for the entire horizon.

Production rates at the four producers (gas, oil and water flows), are given in Fig. 12 for the initial and optimized solution. The ensemble variation, for the optimal production, due to the five reservoir realizations used in the optimization are represented by shaded areas for the 10^{th}-90^{th} and 25^{th}-75^{th} percentile. By comparing the initial and optimized production rates it is clear that the optimization has reduced the amount of produced gas at late times, while at the same time increasing oil production in the early phase. Water production is however increased for all producers. Still, the result is an overall increase in NPV given the chosen market scenario.

The optimization example presented here is a synthetic case assembled to illustrate a field production scenario, which includes several factors that determine the overall performance of upstream oil and gas production in terms of profits vs. cost, such as reservoir flow under uncertainty, multi-phase flow lines, topside process facilities and marked scenarios.

5. Concluding remarks

In this work a set of open-source research tools have been presented for studying integrated planning and optimization of petroleum production scenarios. The functionality of the combined set of tools was demonstrated through numerical examples.

Stable coupling of simulators written in different languages (e.g., MRST and the network simulator) is not straightforward, and in the current work a fully implicit coupling was achieved utilizing the AD-functionality in MRST together with providing Jacobian output-functionality from the network solver. The structure of the full (coupled) system Jacobian, however, is not of a form that easily lends itself to the class

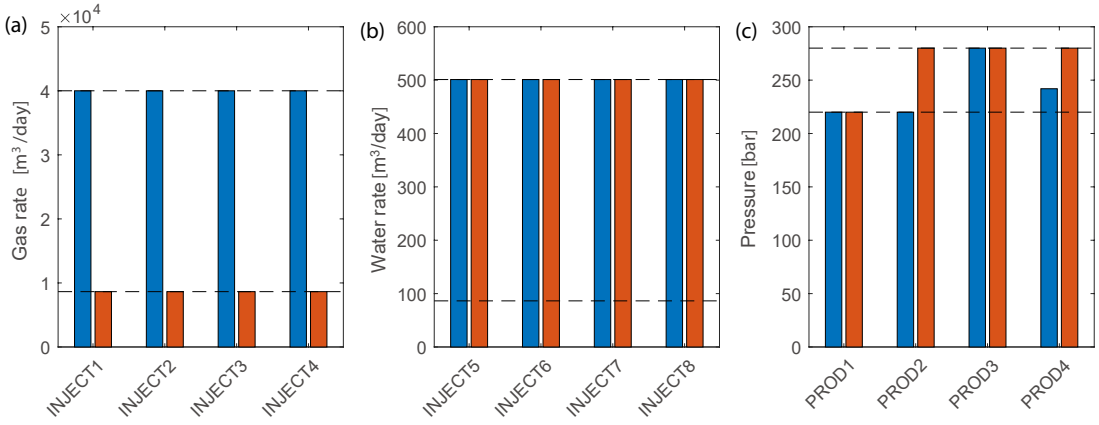

Fig. 11. Optimal controls for first (blue) and second (red) control step. Control bounds are indicated as dashed horizontal lines. Gas injection rates (INJECT 1 to 4), water injection rates (INJECT 5 to 8), and choke pressures (PROD 1 to 4) are given in subfigures (a), (b) and (c), respectively.

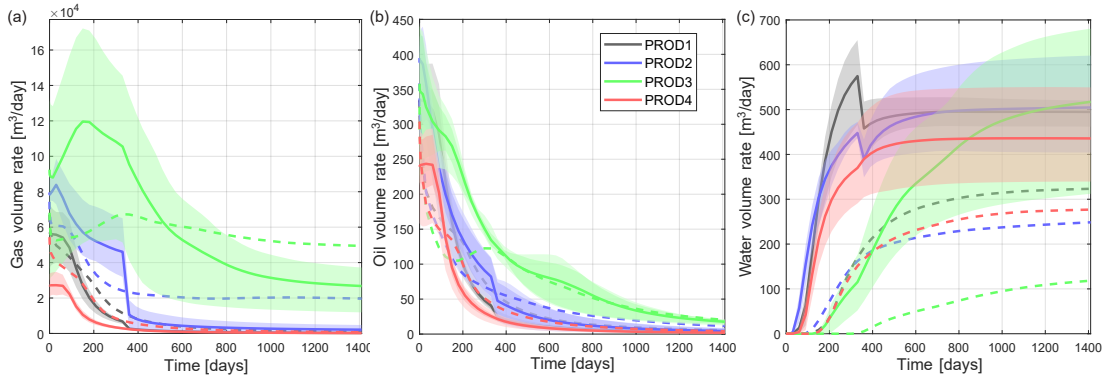

Fig. 12. Initial (dotted line) and optimal (solid lines) production rates at the four producers, given by the (a) gas, (b) oil and (c) water flows. The ensemble variation for the optimal production, due to the five reservoir realizations used in the optimization (as seen in Fig. 6) is given by shaded areas for the 25th-75th percentile.

of linear solvers in MRST, and hence a direct sparse solver was utilized in this work. Setting up coupled model simulation cases requires some domain knowledge and analysis in order to create a feasible system. However, potential users may find the included case creation GUI helpful in this process.

Finally, an obvious improvement to the work presented here would be collecting the functionality in a single coding language. This would improve robustness and efficiency, and make use of adequate linear solvers and e.g., adjoint capabilities more easily attainable.

Acknowledgements

The authors gratefully acknowledge the economic support from The Research Council of Norway and Equinor ASA through *Research Council project 308817 - Digital wells for optimal production and drainage* (DigiWell).

The authors would like to thank the SINTEF colleagues Heiner Schümann, Alv-Arne Grimstad and Per Bergmo at the *Research Council project 296207- Research Centre for a Low-Emission Petroleum Industry on the Norwegian Continental Shelf* (LowEmission), for their contributions to testing of the software, and for giving us valuable feedback and some funding to improve the software.

The authors would also like to thank Caio Giuliani, a researcher with large expertise in derivative-free optimization, who made available the baseline MATLAB implementation of the trust region optimization algorithm used in this work.

Additional information: Author's email

ivareskerud.smith@sintef.no (I. E. Smith).

Supplementary file

https://doi.org/10.46690/ager.2025.03.04

Conflict of interest

The authors declare no competing interest.

References

Bouckaert, S., Pales, A. F., McGlade, C., et al. Net zero by 2050: A roadmap for the global energy sector. Paras,

International Energy Agency, 2021.

Brouwer, D. R., Jansen, J. D. Dynamic optimization of waterflooding with smart wells using optimal control theory. SPE Journal, 2004, 9(4): 391-402.

Bukshtynov, V., Volkov, O., Durlofsky, L. J., et al. Comprehensive framework for gradient-based optimization in closed-loop reservoir management. Computational Geosciences, 2015, 19: 877-897.

Calsep. PVTSim Nova, Calsep, 2024.

Chen, Z. Development of a toolbox for simulation of integrated reservoir-production system. Texas, Texas A&M University, 2020.

Ciaurri, D. E., Mukerji, T., Durlofsky, L. J. Derivative-free optimization for oil field operations, in Computational Optimization and Applications in Engineering and Industry, edited by X. -S. Yang and S. Koziel, Heidelberg, Germany, pp. 19-55, 2011.

Conn, A. R., Gould, N. I., Toint, P. L. Trust Region Methods. Philadelphia, USA, Society for Industrial and Applied Mathematics and Mathematical Programming Society, 2000.

Conn, A. R., Scheinberg, K., Vicente, L. N. Introduction to Derivative-Free Optimization. Philadelphia, USA, Society for Industrial and Applied Mathematics and Mathematical Programming Society, 2009.

da Silva, D. V. A., Jansen, J. D. A review of coupled dynamic well-reservoir simulation. IFAC-PapersOnLine, 2015, 48(6): 236-241.

Guyaguler, B., Zapata, V. J. J., Cao, H., et al. Near-well-subdomain simulations for accurate inflow-performance-relationship calculation to improve stability of reservoir/network coupling. SPE Reservoir Evaluation & Engineering, 2011, 14(5): 634-643.

Hannanu, M. I., Camponogara, E., Silva, T. L., et al. A modified derivative-free SQP-filter trust-region method for uncertainty handling: application in gas-lift optimization. Optimization and Engineering, 2024, https://doi.org/10.1007/s11081-024-09909-0. (in press)

Hannanu, M. I., Silva, T. L., Camponogara, E., et al. Derivative-free well control optimization under uncertainty. Paper Presented at the European Conference on the Mathematics of Geological Reservoirs, 2-5 September, Oslo, Norway, 2024b.

Hoffmann, A., Stanko, M., González, D. Optimized production profile using a coupled reservoir-network model. Journal of Petroleum Exploration and Production Technology, 2019, 9: 2123-2137.

Jansen, J. D. Adjoint-based optimization of multi-phase flow through porous media-a review. Computers & Fluids, 2011, 46(1): 40-51.

Jansen, J. D., Fonseca, R. M., Kahrobaei, S., et al. The egg model-a geological ensemble for reservoir simulation. Geoscience Data Journal, 2014, 1(2): 192-195.

Jelsness, S. Langsiktig kraftmarkedsanalyse 2020-2040. Oslo, The Norwegian Water Resources and Energy Directorate, 2020.

KBC, Multiflash advanced thermodynamics software, KBC, 2024.

Khaledi, H. A., Smith, I. E., Unander, T. E., et al. Investigation of two-phase flow pattern, liquid holdup and pressure drop in viscous oil-gas flow. International Journal of Multiphase Flow, 2014, 67: 37-51.

Kongsberg Digital AS. Advanced mulitphase flow simulator - LedaFLow, 2024.

Kraaijevanger, J. F. B. M., Egberts, P. J. P., Valstar, J. R., et al. Optimal waterflood design using the adjoint method. Paper SPE 105764 Presented at the SPE Reservoir Simulation Symposium, Houston, Texas, 26-28 February, 2007.

Lie, K. -A. An Introduction to Reservoir Simulation Using MATLAB/GNU Octave: User Guide for the MATLAB Reservoir Simulation Toolbox (MRST). Cambridge, UK, Cambridge University Press, 2019.

Lie, K. -A., Krogstad, S. Comparison of two different types of reduced graph-based reservoir models: Interwell networks (GPSNet) versus aggregated coarse-grid networks (CGNet). Geoenergy Science and Engineering, 2023, 221: 111266.

Lie, K. -A., Krogstad, S. Data-driven modelling with coarse-grid network models. Computational Geosciences, 2024, 28(2): 273-287.

Lie, K. -A., Møyner, O. Advanced Modelling with the MATLAB Reservoir Simulation Toolbox. Cambridge, UK, Cambridge University Press, 2021.

Odeh, A. S. Comparison of solutions to a three-dimensional black-oil reservoir simulation problem (includes associated paper 9741). Journal of Petroleum Technology, 1981, 33(1): 13-25.

Redick, B. S., Gildin, E. Improved surface-subsurface coupled reservoir simulation using automatic PID control. IFAC-PapersOnLine, 2018, 51(8): 82-87.

Rasmussen, A. F., Sandve, T. H., Bao, K., et al. The open porous media flow reservoir simulator. Computers & Mathematics with Applications, 2021, 81: 159-185.

Sarma, P., Durlofsky, L. J., Aziz, K., et al. Efficient real-time reservoir management using adjoint-based optimal control and model updating. Computational Geosciences, 2006, 10: 3-36.

Schümann, H., Bergmo, P. Flexible loads in offshore oil and gas production facilities. Oslo, Research Council of Norway, 2022.

Silva, T., Bellout, M., Giuliani, C., et al. A derivative-free trust-region algorithm for well control optimization. Paper Presented at the 17th European Conference on the Mathematics of Oil Recovery, Online Event, 14-17 September, 2020.

Silva, T. L., Bellout, M. C., Giuliani, C., et al. Derivative-free trust region optimization for robust well control under geological uncertainty. Computational Geosciences, 2022, 26(2): 329-349.

SLB. Olga, 2024.

Smith, I. E., Nossen, J., Kjølaas, J., et al. Development of a steady-state point model for prediction of gas/oil and water/oil pipe flow. Journal of Dispersion Science and Technology, 2015, 36(10): 1394-1406.

Statnett. Langsiktig markedsanalyse: Norden og Europa 2020-2050. Oslo, Statnett, 2020.